Received: 20 January 2021 | Revised: 6 August 2021 | Accepted: 30 August 2021

DOI: 10.1002/eng2.12458

RESEARCH ARTICLE

Engineering Reports Open Access WILEY

Effect of organic conditioning layers adsorbed on stainless steel AISI 304 on the attachment and biofilm formation of electroactive bacteria *Shewanella putrefaciens* CN32

Nina Wurzler | **Gundula Hidde** | **Matthias Schenderlein** | **Ozlem Ozcan**

Bundesanstalt für Materialforschung und-prüfung (BAM), Berlin, Germany

Correspondence
Ozlem Ozcan, Bundesanstalt für Materialforschung und-prüfung (BAM), Unter den Eichen 87, 12205 Berlin, Germany.
Email: ozlem.ozcan@bam.de

Abstract

The initial attachment and subsequent biofilm formation of electroactive bacteria *Shewanella putrefaciens* CN32 was investigated to clarify the influence of organic conditioning layers. A selection of macromolecules and self-assembled monolayers (SAMs) of different chain lengths and functional groups were prepared and characterized by means of infrared spectroscopy in terms of their chemistry. Surface energy and Zeta (ζ-) potential of the conditioning layers was determined with contact angle and streaming current measurements. Among the studied surface parameters, a high polar component and a high ratio of polar-to-disperse components of the surface energy has emerged as a successful indicator for the inhibition of the initial settlement of *S. putrefaciens* on stainless steel AISI 304 surfaces. Considering the negative surface charge of planktonic *S. putrefaciens* cells, and the strong inhibition of cell attachment by positively charged polyethylenimine (PEI) conditioning layers, our results indicate that electrostatic interactions do play a subordinate role in controlling the attachment of this microorganism on stainless steel AISI 304 surfaces. For the biofilm formation, the organization of the SAMs affected the local distribution of the biofilms. The formation of three-dimensional and patchy biofilm networks was promoted with increasing disorder of the SAMs.

KEYWORDS

bacterial attachment, conditioning films, self-assembled monolayers, stainless steel

JEL CLASSIFICATION

Materials science

1 | INTRODUCTION

Stainless steels are commonly used as construction material nearly in all industrial applications due to their high corrosion resistance and ability to withstand various environmental stresses. Stainless steel AISI 304 has been widely studied in

terms of its resistance to microbially influenced corrosion (MIC) because of its ability to cope with aggressive and corrosive environments. However, it is vulnerable to pitting corrosion under certain environmental conditions.[1,2]

Bacteria are a ubiquitous part of living mass on earth.[3] As they can attach to, colonize, proliferate and form biofilms on nearly all surfaces, the questions dealing with biofilms and biofilm induced material degradation are of crucial importance to technical, medical and environmental systems.[4] The adhesion and subsequent biofilm formation is a complex physicochemical process initiated by the formation of a surface conditioning film.[1]

The native oxide on stainless steel surfaces is susceptible to contamination. Therefore, a conditioning layer will form immediately when the surface is in contact with natural aqueous environments[1] by the adsorption of molecules present in the surrounding medium or excreted polymeric substances from the bacteria,[5] such as polysaccharides, proteins, lipids, and nucleic acids. Such surface conditioning layers alter the properties of the steel surface significantly.[6]

Despite intensive research efforts, by which mechanisms and to what extent different microorganisms adhere to solid surfaces remained an unanswered question. The chemical and electrochemical properties of the bacterial cell surface and its composition is very heterogeneous,[7–9] and the attachment processes are closely related to the surface chemistry and thermodynamics.[7,10] The outer membrane of gram-negative bacteria is composed of asymmetrically assembled lipopolysaccharides and proteins exposing both phosphoryl- and carboxyl- as well as amine-groups. The neutral pH at incubation conditions leads to spatially heterogeneous surface charges over the cell surface.[11] The chemical heterogeneity of the bacterial cell surfaces present manifold possibilities for interactions with solid surfaces of different functionalities.

The Derjaguin–Landau–Verwey–Overbeek (DLVO) theory addresses several influencing factors for bacterial attachment.[12] Jain and Bhosle analyzed the natural marine conditioning film and the effect of these compounds on the adsorption behavior of three marine bacterial cultures and saw opposing correlation between attachment and the amount of carbohydrates in the conditioning film for three different strains.[13] Lorite et al. investigated the intercorrelation of protein (bovine serum albumin, BSA) adsorption on the attachment behavior and biofilm formation of plant pathogenic bacteria and underlined the important role of the chemical composition of the surface rather than surface roughness and hydrophobicity.[14] The works of Gubner and Beech as well as Pranzetti et al. also supported that the surface hydrophobicity plays a subordinate role.[15,16] Yang et al. applied hyperbranched polymers like branched polyethylenimine (bPEI) for functionalizing the surface of stainless steel AISI 304 for antibacterial applications.[17]

Utilization of self-assembled monolayers (SAMs) as model systems for studying the initial attachment of bacteria to substrata is a well-established strategy. Self-assembled monolayers terminated with hexa-ethylene glycol, methyl, carboxylic acid, and fluorocarbon groups were investigated by phase contrast microscopy by Ista et al. with the conclusion, that different bacterial strains interact very differently with altered wettability characteristics.[18] By systematically varying the physicochemical properties, Khan et al. demonstrated that bacterial attachment is influenced strongly by the surface free energy rather than the wettability of functionalized surfaces.[19] In a combined experimental and modeling study, Liu and Zhao defined the Chen and Qi (CQ) ratio as the ratio of disperse to polar components of the surface energy. They reported that for Ni-P-PTFE coatings, the attachment of *Pseudomonas fluorescens, Cobetia marina* and *Vibrio alginolyticus* decreased with decreasing CQ ratio.[20] Raman and Gawalt pointed out, that a lot of work on functionalizing surfaces for biomedical applications and antifouling strategies has been performed on model substrates, but only a few papers applying SAMs to stainless steel can be found in literature, even less on studying the SAM's influence on bacterial attachment.[21] This aspect is especially crucial, as the chain length and the headgroup of the monolayer molecule has an influence on the electrochemical activity of electroactive bacteria via electron transfer mediation,[22] having possible impact on the MIC processes.

Shewanella putrefaciens is a facultative anaerobic microorganism, capable of utilizing various compounds present in the protective passive film on stainless steel surfaces, such as Fe(III), Mn(IV), and Cr(VI) among other inorganic/organic compounds as electron acceptor.[23–26] The *Shewanella* species as member of dissimilatory iron reducing bacteria (DIRB) gained attention in different research areas due to their ability of metal reduction for bioremediation or biodegradation[27,28] as well as a threat in microbially influenced corrosion (MIC) to steel constructs submerged in natural environments.[29,30] In addition to the microbe's ability to influence the corrosion behavior of steel directly, the patchy deposits of natural biofilms can establish local regions of different surface potentials facilitating corrosion processes.[31]

The objective of this study was to elucidate a potential correlation between various properties of the conditioning layers formed on stainless steel AISI 304 surfaces and the attachment of *S. putrefaciens* CN32. *S. putrefaciens* CN32 was selected in this study as a model microorganism due to its abundance in natural environments and its relevance to microbially influenced corrosion (MIC).[32] Polyethylenimine (PEI) and humic acids (HA) were investigated as macromolecular

conditioning layers. PEI has a high density of amine groups and is therefore widely used in many industrial applications[33] and is thus a common contaminant in water treatment making it probable to spontaneously occur in process waters in contact with stainless steel AISI 304.[33,34] Humic acids were chosen to provide a realistic scenario resembling sediment conditions.[35] As they are formed during degradation of organic matter, humic acids account for the majority of dissolved organic carbon in water.[36] Additionally, four SAMs with different surface charges, varying chain length and changes in chemical functionality were included into the study as model substrates, as their surface properties can be precisely characterized. By combining a detailed surface characterization with the investigation of the attachment behavior of *S. putrefaciens* CN32, the effect of different surface characteristics of the conditioning films on the initial bacterial settlement and biofilm formation has been evaluated.

2 | MATERIALS AND METHODS

2.1 | Sample preparation

Stainless steel AISI 304 coupons were ground to P4000 with silicon carbide paper, ultrasonically cleaned in pure acetone for 10 min and electrochemically preconditioned in $NaClO_4$ (20 mM) at +50 mV versus OCP (Ag/AgCl 3 M NaCl and gold wire electrodes [Gamry 600+ potentiostat, C3 Prozessanalytik, Germany]) for 60 min. to create a thin and reproducible oxide layer on all substrates.[37]

Polyethylenimine (PEI, branched, H-$[NHCH_2CH_2]_n$-NH_2, MW: 25000 mol g^{-1}, Sigma Aldrich) and humic acid (native, MW: n.a., Carl ROTH) were dissolved in 70% isopropanol to a concentration of 1 mM and 4.3 mg L^{-1}, respectively.[38] The macromolecule conditioning layers will be referred to as PEI and humic in the manuscript text.

Following molecules were used for SAM surface functionalization: Oleic acid (oleic, CH_3-$[CH_2]_{15}$-COOH, MW: 282.52 g mol^{-1}, 99% purity, abcr), 3-aminopropylphosphonic acid (APPA, NH_3-$(CH_2)_3$-$PO(OH)_2$, MW: 139.09 g mol^{-1}, 98% purity, Fluorochem, Ltd.), octadecylphosphonic acid (ODPA, CH_3-$(CH_2)_{17}$-$PO(OH)_2$, MW: 334.47 g mol^{-1}, 97% purity, Carl ROTH) and 16-hydroxyhexadecanoic acid (hydroxic, OH-$(CH_2)_{16}$-COOH, MW: 272.42 g mol^{-1}, 98% purity, Sigma Aldrich). One millimolar solutions were prepared with 70% vol. iso-propanol in water as solvent.

2.2 | Characterization of the conditioning layers

Fourier-Transform-infrared (FT-IR) spectroscopy measurements were performed using a Nicolet 8700 FTIR spectrometer (Thermo Fisher Scientific, Inc., USA) equipped with a variable angle VeeMAX III external reflection accessory. A reflection angle of 80° was used for higher surface sensitivity. For the acquisition of single beam spectra, 512 scans were accumulatively collected in a wavenumber range of 800–4000 cm^{-1} with a 4 cm^{-1} spectral resolution. To visualize the adsorption and assembly of molecules, ex situ absorbance spectra were calculated using the pure steel sample as the reference. Atmospheric correction and base line adjustment were performed manually.

Contact angle measurements and determination of the surface energies were performed on a Drop Shape Analyzer DSA30 (KRÜSS GmbH, Hamburg, Germany) with ADVANCE software (Version 1.6.2.0). Water, ethylene glycol and di-iodomethane were used for contact angle measurements. More details on the calculation of the energy components can be found in the Appendix S1.

The Zeta (ζ)-potential is the surface potential measured at the shear plane of the electrolyte over the surface and is considered to give insights into the attractive and repulsive forces that can play a major role in the interaction mechanisms between bacteria and surfaces upon adsorption. Zeta (ζ)-potential measurements were carried out with a SurPass electrokinetic analyzer (Anton Paar, Germany) in a clamp cell. The investigated substrate was covered with a spacer foil leaving a test area of 5 cm × 0.8 cm × 100 µm free as a flow channel. On top of the spacer foil, a reference polypropylene-foil was placed, and the cell was sealed and placed in the sample holder. The streaming potential as a function of pressure was recorded by pumping an electrolyte (20 mM $NaClO_4$) four times back and forth through the sample gap at applied pressures up to 400 mbar. From the streaming potential values, the Zeta (ζ)-potential was calculated using the Helmholtz–Smoluchowski equation for planar, conductive substrates.[39] For each substrate a single-point measurement was performed at the pH value of the incubation medium (pH 7) followed by a titration procedure from pH 11 to pH 4.

2.3 | Preparation of cell suspensions for attachment experiments

In order to eliminate various factors as different growth phases or changing environmental factors during investigation of MIC, a chemostat was installed, maintaining the bacterial culture at a set A_{600} of 0.1 and growth state. The chemostat was placed in a temperature-controlled water bath on a magnetic stirrer and continuously bubbled with sterile air. A feed solution of sterile minimal medium (ShMM–*Shewanella* minimal medium [see Table SI.1, adapted from M9 minimal medium, Miller et al.[40]]) with 40 mM lactate was pumped at a flowrate of 167 µl min^{-1}. A drain was installed to prevent overflow and acted as waste material outlet.

Dynamic light scattering (DLS) (Zetasizer Ver. 7.13, Malvern Instruments, Ltd.) was used to measure the surface Zeta (ζ)-potential of the bacterial cells in both, minimal growth medium ShMM as well as 20 mM $NaClO_4$. An average was built from 12 runs in each of the 5 repetitions.

2.4 | Investigation of the attachment behavior

For studying the initial irreversible attachment, 1 h of incubation with the bacterial solution was performed. The substrates with different conditioning layers were placed in sterile containers and statically incubated with fresh minimal medium mixed 1:1 with the bacterial solution from a continuous culture (final $A_{600} = 0.05$). After 1 h, the samples were washed in stirring water for 10 s, followed by a 4′,6-diamidin-2-phenylindol (DAPI) staining procedure. In the staining procedure, samples were gently washed in tris(hydroxymethyl)aminomethan (TRIS) buffer solution at pH 7.4 and then placed in 6-well plates. Each sample was covered with a mixture of TRIS buffer solution and DAPI stain stock solution 1 mg ml^{-1} at a concentration 1000:1 and incubated at 4°C for 30 min in the dark. After gently washing the samples, they were pre dried in the laminar flow of the sterile bench in dark, fixated with mount floor, and covered with glass slips. Samples were kept in dark until fluorescence imaging.

Five images per sample were collected in a predefined pattern to eliminate subjective analysis (details can be found in Figures SI.1 and SI.2). A fluorescence microscope (Nikon H550L eclipse, ×40 objective) was used for cell counting. Cell counting was performed over 15 images per sample system with ImageJ by particle count method after binary transformation of the images and setting a color threshold. The analysis was performed in triplicates to assure reproducibility.

For the investigation of biofilm formation, SEM micrographs were taken after 20 h incubation experiments. For the SEM analysis, the samples were fixated in a 2.5% glutaraldehyde solution for 4 h at 4°C (diluted 25% for electron Microscopy, Merck, Germany) followed by washing in ddH_2O for 5 min and subsequent dehydration in an ethanol series (gradually increasing alcohol of 30%, 50%, 70%, 80%, 90%, and 100% [twice], each step for 15 min.) before imaging.[41] SEM imaging was performed on a Zeiss SEM Evo MA10 operated at 10 kV accelerating voltage in SE mode at 7×10^{-5} mbar vacuum.

3 | RESULTS AND DISCUSSION

3.1 | Characterization of the conditioning layers

The adsorption of the macromolecular conditioning layers was confirmed by means of FTIR analysis (Figure 1). The IR spectra after adsorption of PEI indicate an amine rich surface film with strong C=C vibrations, which indicate the presence of a thick adsorption layer. The unknown substances grouped up in humic acids prevent a distinct identification of single functionalities in IR spectra, however, a high amount of amine groups as well as phosphates and carbon chains are clearly visible. At 1620 cm^{-1} aromatic C=C vibrations and C=O stretching of the H-bond quinones have been identified.[36]

The IR spectra of the SAMs (Figure 2B) are showing peaks characteristic for the CH_3/CH_2 backbone (2813–2950 cm^{-1}).[42] Oleic acid molecules adsorbed on the surface in a disorganized structure given by the suppressed and broader IR peaks in this region. This can be explained with the presence of the *cis* double bond between C9=C10 causing steric hindrance of the molecules preventing the formation of a self-assembled monolayer with high order.[43] The region around 1700 cm^{-1} assigned to carboxylic acid species points to a preferential adsorption of the carboxylic group onto the steel surface, leaving the CH_3 group as the terminal group.[44] For hydroxic SAMs, the $\nu_{as}CH_2$ shifted to lower wavenumbers at 2918 cm^{-1} as a result of the well-ordered film of the alkyl chains which is a sign for a common tilt angle of all the

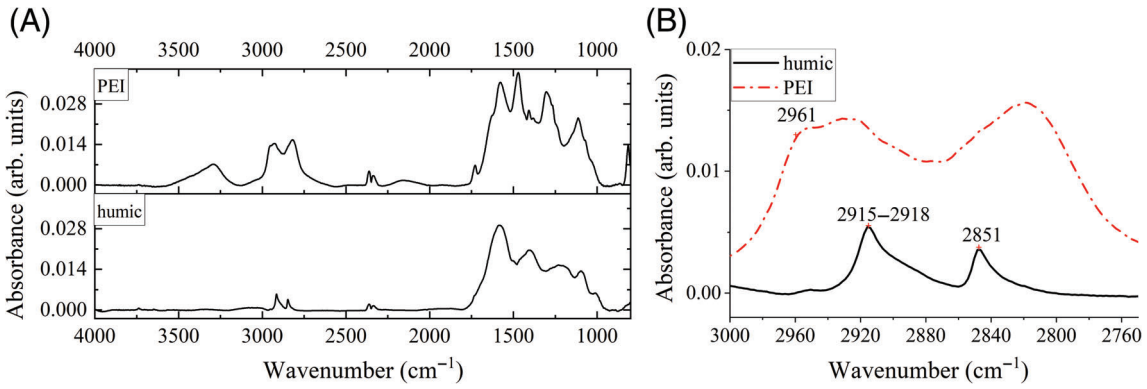

FIGURE 1 FTIR spectra of macromolecules PEI and humic acids adsorbed from isopropanol (70% in ddH_2O) onto stainless steel AISI 304 after 20 h, (A) whole recorded range, (B) enlarged carbon chain backbone peaks

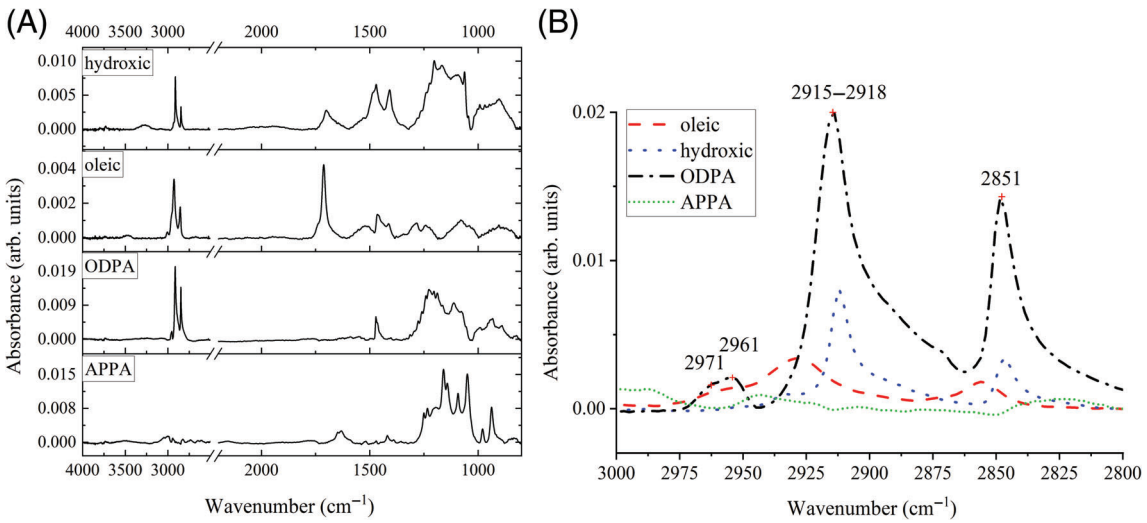

FIGURE 2 FTIR spectra of adsorbed SAMs adsorbed from isopropanol (70% in ddH_2O) onto stainless steel AISI 304 after 20 h, (A) whole recorded range, (B) enlarged carbon chain backbone peaks

adsorbed molecules in an all-trans configuration.[21,45] The films of APPA on stainless steel AISI 304 surfaces do not exhibit high intensities in the CH_3/CH_2 region due to the short chain length, however, can be identified in the fingerprint region. The HO—P=O peak at 1620 cm^{-1} and the high intensity for P=O implies that the adsorption of APPA is a tail-to-surface adsorption with the phosphate group being the terminal end. The fingerprint region of the ODPA SAM spectra adsorbed to the steel substrate give evidence for a mixed mono- and bidentate adsorption state.[46,47] Moreover, the peak frequencies of out-of-plane, in-plane $\nu_{as}CH_3$ at 2961 and 2971 cm^{-1} are quite intense compared to other SAMs in this study.[48] These findings imply the monolayer of ODPA behaves as a compact well-ordered SAM.

3.2 | Effect of the conditioning layers on surface charge and wettability

The measured surface Zeta (ζ)-potentials are presented in Figure 3A,B. Stainless steel AISI 304 surfaces prior to the adsorption of conditioning layers (pure) have shown an isoelectric point (IEP) at ~ pH 6.4. As stated in the literature, PEI functionalized surfaces have a high positive charge within the whole pH range due to the presence of amine functionalities.[49] The observed negative surface charge for the humic acid coated surface in the alkaline conditions could be explained with the presence of —COOH and —OH functional groups.[50] At incubation conditions (pH 7), the ODPA SAMs are at their isoelectric point (IEP), and therefore show a neutral net charge. Hydroxic and oleic SAMs showed a

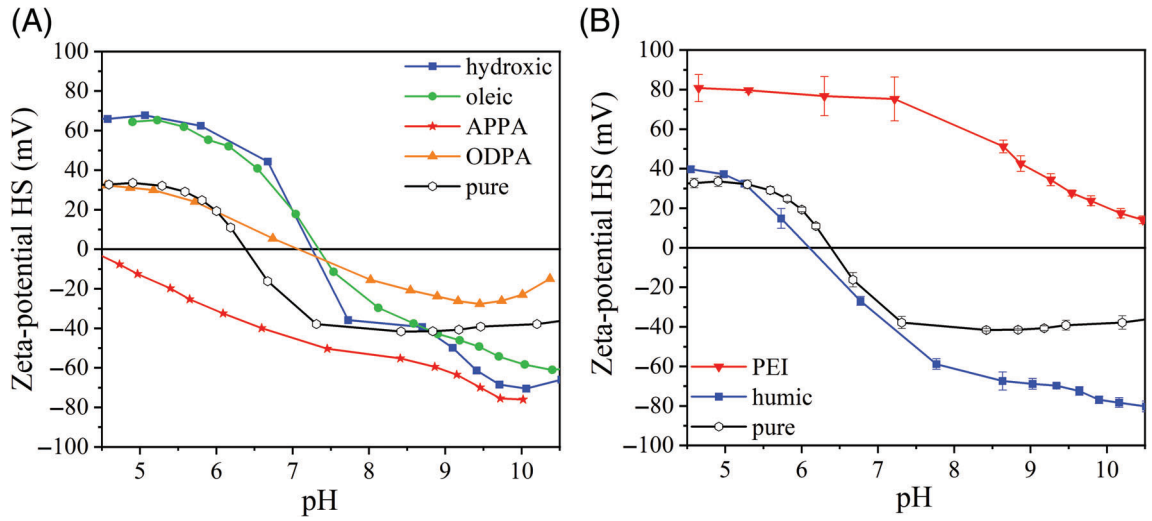

FIGURE 3 Surface Zeta (ζ)-potentials determined by means of streaming potential in $NaClO_4$ (20 mM), (A) SAMs and pure stainless steel AISI 304, (B) macromolecules and pure stainless steel AISI 304

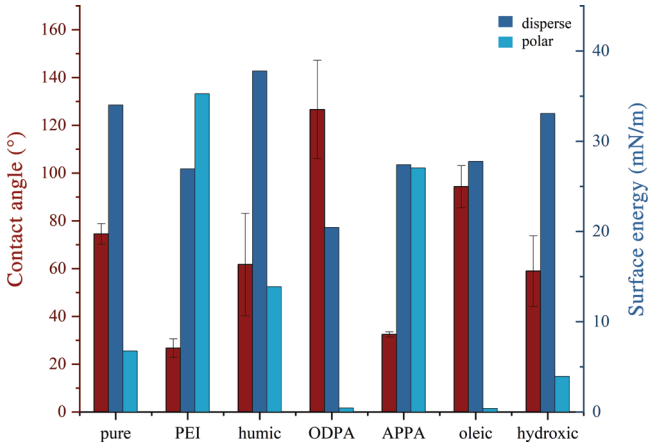

FIGURE 4 Contact angle measurements and surface energy determination of the formed conditioning layers as described in Appendix S1 Equations (1)–(3)

very similar behavior with an isoelectric point at ~ pH 7.3. The adsorption of short chained APPA led to a negative surface charge in the whole pH-range agreeing well with the adsorption via the amine functionality, which resulted in a strong negative Zeta (ζ)-potential deriving from the phosphonate terminal end.

Contact angle measurements give insight into the wetting behavior of solid surfaces. The stainless steel AISI 304 surfaces without conditioning layers showed a water contact angle of about 70°, indicating a slightly hydrophilic surface (Figure 4). The influence of —NH_3 groups on the water contact angle was strongly pronounced in PEI, which had the lowest water contact angle and the highest polar component of the surface energies. The heterogeneous nature of humic acid conditioning layers resulted in an overall hydrophilic behavior with very high surface energies in comparison to untreated stainless steel AISI 304. The disperse component of the surface energy of humic acid film was the highest value observed in this study.

ODPA SAMs showed the highest water contact angle, originating from the —CH_3 terminated, highly-ordered monolayer. Both surface energy components were suppressed, and the polar component was almost nonexisting. The water contact angle of oleic SAMs was ~90° with an increase compared to the pure substrate originating from the —CH_3 tail groups. However, the disorder of the oleic SAMs, as evidenced by FTIR analysis resulted in a much lower contact angle than ODPA SAMs. The polar and disperse parts of the surface energy of oleic surfaces diverged widely with an almost negligible polar component, similar to ODPA SAMs. As the pure steel surface is rich in hydroxyl groups, the adsorption

of hydroxyl-terminated SAMs only led to a decrease in the water contact angle without any significant changes in the surface energy components. APPA's low water contact angle indicated a hydrophilic surface caused by the influence of the phosphate groups and both components of the surface energy were high and equally distributed.

3.3 | Primary irreversible attachment and biofilm formation

In the study of the attachment behavior of *S. putrefaciens* CN32, the primary irreversible settlement phase (1 h incubation) was investigated optically by means of fluorescence imaging and subsequent cell counting (for more information on the procedures, see Figures SI.1 and SI.2). To correlate the general surface charge of *S. putrefaciens* cells with their attachment behavior, DLS analysis was performed with cell suspensions. DLS measurements indicated a negative ζ-potential of -7.3 ± 0.8 and -14.6 ± 1.9 mV for planktonic *S. putrefaciens* cells suspended in ShMM and $NaClO_4$, respectively. The measured ζ-potential values of the *S. putrefaciens* agree well with literature where a negative surface charge density of $\sim -23\ \mu C/cm^2$ at pH 7 was previously reported.[51]

In Figure 5A the coverage of bacteria is presented in percent of the available surface area. After 1 h initial attachment, all conditioning layers have resulted in fewer adhered cells in comparison to the pure stainless steel AISI 304 substrates. The highest affinity of the bacteria among the SAM conditioning layers was observed with surfaces functionalized with oleic and hydroxic SAMs followed by ODPA and APPA.

The attachment behavior differs significantly between the conditioning layers formed by macromolecules. The highly positively charged, thick and viscous PEI layer was the least attractive surface conditioning film and efficiently inhibited the attachment of *S. putrefaciens*. The humic acid components were covering the surface very heterogeneously leading to a high variation in attachment behavior and a high standard deviation. In the literature, the least attractive surface energy in the Baier curve was reported to be in the range of 20–30 mN/m.[52] In the present study, both ODPA and oleic SAMs exhibit these values, however, the lowest inhibition effect was observed with surfaces functionalized with oleic acid SAMs.

In Figure 5B, the correlation between the polar component of the surface energy and the adhesion of cells within the first hour of incubation is depicted. The polar component of the surface energy and a higher ratio of the polar to dispersed component (a low CQ ratio[20,53]) crystallized as an essential factor in this work. However, contrary to the observations of Liu and Zhao,[20] with the organic conditioning layers investigated in this work, no direct correlation of CQ ratio and bacterial coverage was observed until values of ≤1.0 were reached. This controversy can be explained by the fact that in their work other surface properties were kept nearly constant using Ni-P-PTFE coatings. Nevertheless, our results from the *S. putrefaciens* CN32 – stainless steel AISI 304 system support the concept presented by Liu and Zhao[20] that a low CQ ratio is crucial for the design of novel antifouling strategies.

Figure 6 gives an overview about surface properties and indicators that were investigated in this study together with the percentage of bacterial coverage after 1 h of incubation. For similar values in coverage, a group can be formed of oleic, hydroxic, and ODPA SAMs, all presenting a low total surface energy, a low polar component and a low ratio of polar

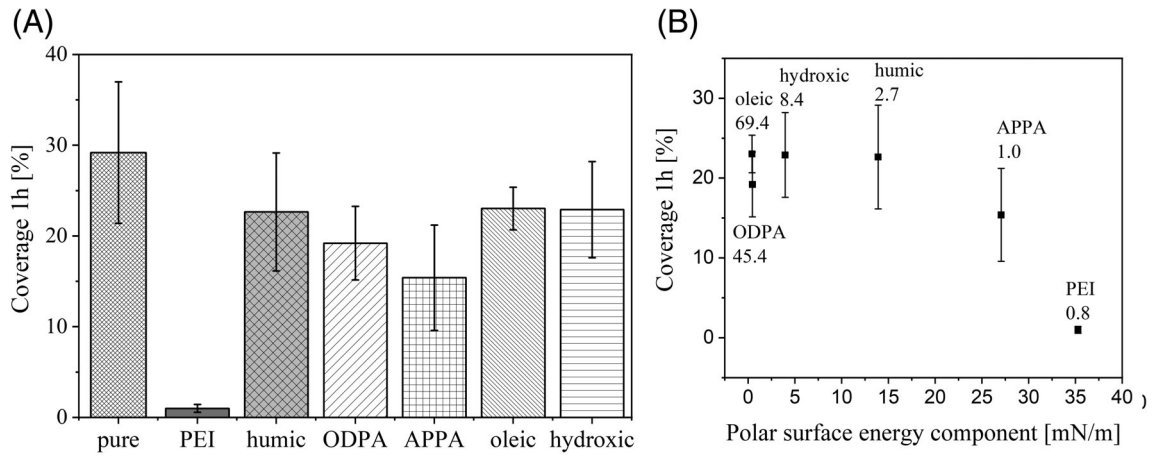

FIGURE 5 (A) surface coverage by bacterial cells in % after 1 h of incubation, (B) coverage after 1 h in relation to polar component of surface energy with insets of CQ-ratio[20] for each surface

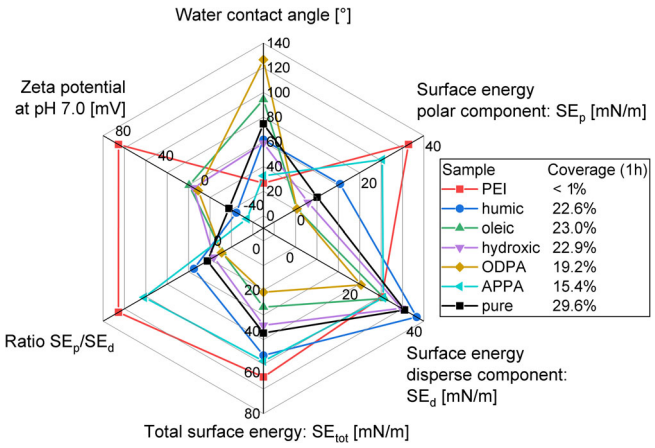

FIGURE 6 Summary of all measured surface properties of the conditioning layers and the initial bacterial coverage

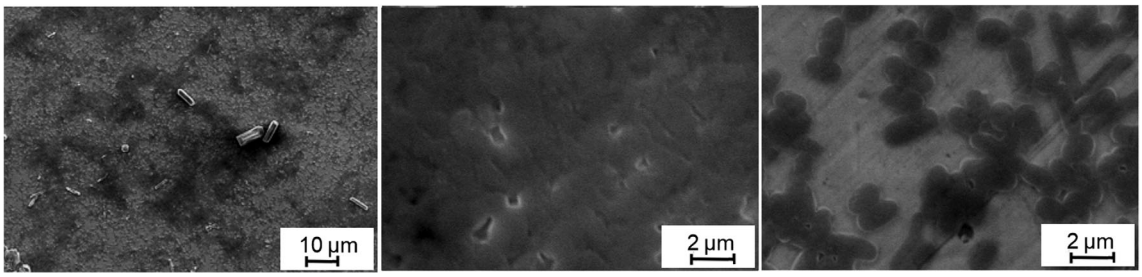

FIGURE 7 SEM images collected after 20 h incubation in *Shewanella putrefaciens* CN32 on the stainless steel AISI 304 without the adsorption of conditioning layers at low (A) and high (B, C) magnification

to disperse part as well as a low surface charge seen by the bacteria. The very different contact angles did not have a significant impact on bacterial attachment. Considering that the adsorption of SAMs does not alter the surface roughness and generates a homogeneous film, the wettability of the surfaces can be discarded as an important factor in the initial attachment for the studied microorganism/substrate system. Furthermore, at incubation conditions (pH 7.0), APPA and PEI covered stainless steel AISI 304 surfaces exhibited very strong negative and positive surface charges, respectively. Considering the negative surface charge of planktonic *S. putrefaciens* cells, based on electrostatic interactions, APPA covered surfaces would be expected to lead to repulsive effects inhibiting the settlement of bacterial cells. However, our results demonstrate an opposite effect, where adsorbed PEI films with very high positive charge led to a clear inhibition of bacterial settlement indicating that electrostatic interactions do not play a significant role in controlling the initial attachment of *S. putrefaciens* cells on stainless steel AISI 304 substrates.

After overcoming the initial attachment phase, the bacteria settle down in greater numbers and start to build a biofilm. In Figure 7 the SEM images of the biofilms formed on stainless steel AISI 304 surfaces without the adsorption of conditioning layers (pure) are presented. The darker regions in Figure 7A are covered with a dense and three-dimensional biofilm (Figure 7B), whereas the lighter areas are characterized by sparsely distributed singular cells as seen in and Figure 7C, respectively.

The SEM images of the biofilms formed after 20 h of incubation on conditioning layer covered stainless steel AISI 304 surfaces are presented in Figure 8. Despite the prolonged incubation, PEI covered surfaces showed nearly no bacterial colonization and an effective inhibition of biofilm formation. Oppositely, humic substrates progressed with complete but very inhomogeneous coverage with higher three-dimensional biofilm buildups, which can be explained with the presence of soluble and nonsoluble components with higher electronic conductivity. *S. putrefaciens* belongs to iron reducing bacteria capable of performing indirect electron transfer with metallic surfaces utilizing electron conducting paths offered by humic acid conditioning layers. Thus, the presence of conducting and nonconducting film constituents in the humic acid conditioning film might explain the patchy and three-dimensional structure of the biofilms.

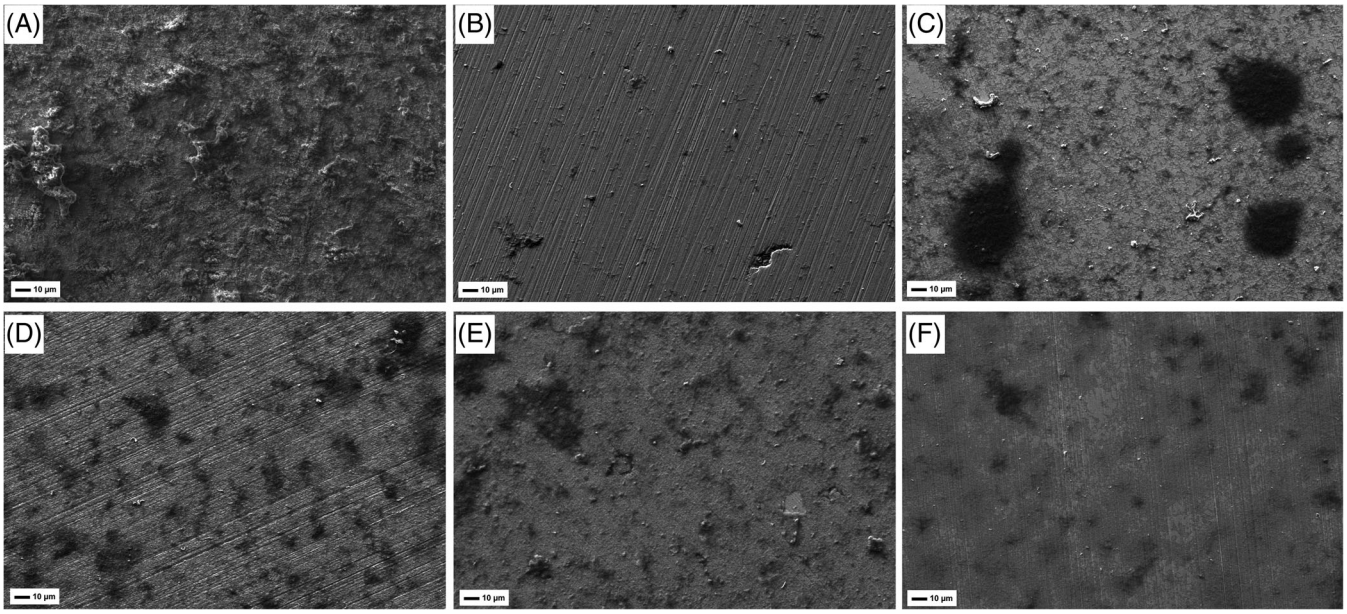

FIGURE 8 SEM images collected after 20 h incubation with *Shewanella putrefaciens* CN32 on conditioning layers at 10 kV, (A) humic, (B) PEI, (C) oleic, (D) hydroxic, (E) ODPA, (F) APPA

Oleic acids initial uniform attraction has evolved into a highly differentiated/island-like attachment pattern. Hydroxic functionalized surfaces showed a mixture of small patches of biofilms together with well dispersed singular cells. ODPA exhibits a uniform and thicker biofilm formation. APPA SAMs on the other hand led to evenly distributed attached bacterial cells with low EPS production. On SAM functionalized surfaces, the presence of defects as indicated by lower degree of organization observed in infrared spectra, can lead to the formation of local defect sites. These can facilitate electron transfer during longer incubation times and promote localized biofilm formation. This trend is visible in the SEM images when comparing ODPA, hydroxic acid, and oleic acid functionalized surfaces, where the latter with the least ordered structure led to formation of heterogeneous biofilms. Thus, our results indicate that for SAMs that have been chosen to represent model short-chain organic thin films in this work, the biofilm formation behavior of *S. putrefaciens* on stainless steel AISI 304 can be affected by the long-term integrity of the SAMs and their ability of blocking the electron transfer on the metal surface.

4 | CONCLUSION

This article reports the investigation of SAMs and macromolecules with a range of wettability, surface energies, chemical composition, and surface charge as conditioning layers to determine the attachment and biofilm formation behavior of electroactive bacteria *S. putrefaciens* CN32 on stainless steel AISI 304.

Following conclusions can be drawn for the studied microorganism and substrate:

- The strongest correlation for the inhibition of initial settlement was observed with the polar component of the surface energy. Moreover, a high polar-to-disperse ratio (a low CQ-ratio[20]) indicated a higher inhibition of initial bacterial settlement.
- Surface wettability and electrostatic interactions have a subordinate role for the studied conditioning layers in predicting the initial settlement of *S. putrefaciens* on stainless steel AISI 304.
- The high density of the formed biofilms on humic acid conditioning layers, as well as the differences in biofilm heterogeneity observed with SAMs of different molecular ordering indicates that electrochemical interactions between the electroactive bacteria and the substrate could play a major role in controlling the biofilm formation.

- Further research shall focus on the application of high-resolution methods, especially on the stability of the SAMs under incubation conditions and on the electroconductivity of these conditioning films to clarify the processes leading to localized biofilm growth.

ACKNOWLEDGMENTS

The authors gratefully acknowledge Jan David Schütter for productive discussions. Open Access funding enabled and organized by Projekt DEAL.

CONFLICT OF INTEREST

The authors declare no potential conflict of interest.

AUTHOR CONTRIBUTIONS

Nina Wurzler: Conceptualization (supporting); formal analysis (lead); investigation (lead); methodology (lead); visualization (lead); writing – original draft (lead); writing – review and editing (equal). **Gundula Hidde:** Formal analysis (supporting); investigation (supporting); writing – review and editing (supporting). **Matthias Schenderlein:** Conceptualization (supporting); investigation (supporting); methodology (supporting); writing – review and editing (supporting). **Ozlem Ozcan:** Conceptualization (lead); methodology (supporting); supervision (lead); visualization (supporting); writing – original draft (supporting); writing – review and editing (equal).

DATA AVAILABILITY STATEMENT

The data that supports the methods and results of this study are available in the supporting information of this article. Further data that support the findings of this study are available from the corresponding author upon reasonable request.

ORCID

Ozlem Ozcan https://orcid.org/0000-0002-7457-4985

REFERENCES

1. Hocevar M, Jenko M, Godec M, Drobne D. An overview of the influence of stainless-steel surface properties on bacterial adhesion. *Mater Technol*. 2014;48(5):609-616.
2. Lundin M, Hedberg Y, Jiang T, et al. Adsorption and protein-induced metal release from chromium metal and stainless steel. *J Colloid Interface Sci*. 2012;366:155-164.
3. Coetser SE, Cloete TE. Biofouling and biocorrosion in industrial water systems. *Crit Rev Microbiol*. 2005;31(4):213-232. https://doi.org/10.1080/10408410500304074
4. Li K, Whitfield M, Van Vliet KJ. Beating the bugs: roles of microbial biofilms in corrosion. *Corros Rev*. 2013;31(3–6):73–84. https://doi.org/10.1515/corrrev-2013-0019
5. Beech IB. Corrosion of technical materials in the presence of biofilms—current understanding and state-of-the art methods of study. *Int Biodeter Biodegr*. 2004;53(3):177-183. https://doi.org/10.1016/s0964-8305(03)00092-1
6. Liu H, Gu T, Asif M, Zhang G, Liu H. The corrosion behavior and mechanism of carbon steel induced by extracellular polymeric substances of iron-oxidizing bacteria. *Corros Sci*. 2017;114:102-111. https://doi.org/10.1016/j.corsci.2016.10.025
7. Korenevsky A, Beveridge TJ. The surface physicochemistry and adhesiveness of *Shewanella* are affected by their surface polysaccharides. *Microbiology*. 2007;153:1872-1883.
8. Korenevsky AA, Vinogradov E, Gorby Y, Beveridge TJ. Characterization of the lipopolysaccharides and capsules of Shewanella spp. *Appl Environ Microbiol*. 2002;68(9):4653-4657. https://doi.org/10.1128/aem.68.9.4653-4657.2002
9. Sokolov I, Smith DS, Henderson GS, Gorby YA, Ferris FG. Cell surface electrochemical heterogeneity of the Fe(III)-reducing Bacteria*Shewanella putrefaciens*. *Environ Sci Technol*. 2001;35(2):341-347. https://doi.org/10.1021/es001258s
10. Jacobs A, Lafolie F, Herry JM, Debroux M. Kinetic adhesion of bacterial cells to sand: cell surface properties and adhesion rate. *Colloids Surf B Biointerfaces*. 2007;59:35-45.
11. Sokolov I, Smith DS, Henderson GS, Gorby Y, Ferris FG. Cell surface electrochemical heterogeneity of the Fe(III)-reducing bacteria *Shewanella putrefaciens*. *Environ Sci Technol*. 2001;35:341-347.
12. Hermansson M. The DLVO theory in microbial adhesion. *Colloids Surf B Biointerfaces*. 1999;14:105-119. https://doi.org/10.1016/S0927-7765(99)00029-6
13. Jain A, Bhosle NB. Biochemical composition of the marine conditioning film: implications for bacterial adhesion. *Biofouling*. 2009;25(1):13-19.
14. Lorite GS, Rodrigues CM, de Souza AA, Kranz C, Mizaikoff B, Cotta MA. The role of conditioning film formation and surface chemical chaned on *Xylella fastidiosa* adhesion and biofilm evolution. *J Colloid Interface Sci*. 2011;359:289-295. https://doi.org/10.1016/j.jcis.2011.03.066

15. Gubner R, Beech IB. The effect of extracellular polymeric substances on the attachment of pseudomonas NCIMB 2021 to AISI 304 and 316 stainless steel. *Biofouling*. 2000;15:25-36.
16. Pranzetti A, Salaün S, Mieszkin S, et al. Model organic surfaces to probe marine bacterial adhesion kinetics by surface Plasmon resonance. *Adv Funct Mater*. 2012;22:3672-3681.
17. Yang WJ, Neoh K-G, Kang E-T, Teo SL-M, Rittschof D. Stainless steel surfaces with thiol-terminated hyperbranched polymers for functionalization via thiol-based chemistry. *Polym Chem*. 2013;4:3105-3115. https://doi.org/10.1039/C3PY00009E
18. Ista LK, Fan H, Baca O, López GP. Attachment of bacteria to model solid surfaces:oligo(ethylene glycol) surfaces inhibit bacterial attachment. *FEMS Microbiol Lett*. 1996;142:59-63.
19. Khan MT, Ista LK, Lopéz GP, Schuler AJ. Experimental and theoretical examination of surface energy and adhesion of nitrifying and heterotrophic bacteria using self-assembled monolayers. *Environ Sci Technol*. 2011;45:1055-1060.
20. Liu C, Zhao Q. The CQ ratio of surface energy components influences adhesion and removal of fouling bacteria. *Biofouling*. 2011;27(3):275-285. https://doi.org/10.1080/08927014.2011.563842
21. Raman A, Gawalt ES. Self-assembled monolayers of alkanoic acids on the native oxide surface of SS316L by solution deposition. *Langmuir*. 2007;23(5):2284-2288. https://doi.org/10.1021/la063089g
22. Crittenden SR, Sund CJ, Sumner JJ. Mediating electron transfer from bacteria to a gold electrode via a self-assembled monolayer. *Langmuire*. 2006;22(23):9473-9476. https://doi.org/10.1021/la061869j
23. Marsili E, Baron DB, Shikhare ID, Coursolle D, Gralnick JA, Bond DR. Shewanella secretes flavins that mediate extracellular electron transfer. *Proc Nat Acad Sci*. 2008;105(10):3968-3973. https://doi.org/10.1073/pnas.0710525105
24. Fredrickson JK, Romine MF, Beliaev AS, et al. Towards environmental systems biology of Shewanella. *Nat Rev Microbiol*. 2008;6(8):592-603. https://doi.org/10.1038/nrmicro1947
25. Lovley DR. The microbe electric: conversion of organic matter to electricity. *Curr Opin Biotechnol*. 2008;19(6):564-571. https://doi.org/10.1016/j.copbio.2008.10.005
26. Carmona-Martínez AA, Harnisch F, Kuhlicke U, Neu TR, Schröder U. Electron transfer and biofilm formation of *Shewanella putrefaciens* as function of anode potential. *Bioelectrochemistry*. 2013;93:23-29. https://doi.org/10.1016/j.bioelechem.2012.05.002
27. Zhu W, Wang R, Huang T, Wu F. The characteristics and two-step reaction model of p-nitroacetophenone biodegradation mediated by *Shewanella decolorationis* S12 and electron shuttle in the presence/absence of goethite. *Environ Technol*. 2014;35(21–24):3116-3123. https://doi.org/10.1080/09593330.2014.931471
28. Zhu W, Nan Y, Huang T, Wu F. The mechanism, thermodynamic and kinetic characteristics of the microbial reduction of goethite mediated by Anthraquinone-2-Sulfonate. *Geomicrobiol J*. 2013;30(10):928-940. https://doi.org/10.1080/01490451.2013.791356
29. Herrera LK, Videla HA. Role of iron-reducing bacteria in corrosion and protection of carbon steel. *Int Biodeter Biodegr*. 2009;63(7):891-895. https://doi.org/10.1016/j.ibiod.2009.06.003
30. Videla HA, Herrera LK. Microbiologically influenced corrosion: looking to the future. *Int Microbiol*. 2005;8:169-180.
31. Dubiel M, Hsu CH, Chien CC, Mansfeld F, Newman DK. Microbial iron respiration can protect steel from corrosion. *Appl Environ Microbiol*. 2002;68(3):1440-1445. https://doi.org/10.1128/aem.68.3.1440-1445.2002
32. Wurzler N, Schutter JD, Wagner R, Dimper M, Lützenkirchen-Hecht D, Ozcan O. Abundance of Fe(III) during cultivation affects the microbiologically influenced corrosion (MIC) behaviour of iron reducing bacteria *Shewanella putrefaciens*. *Corros Sci*. 2020;174:108855-1–108855-8. https://doi.org/10.1016/j.corsci.2020.108855
33. Wen S, Zheng F, Shen M, Shi X. Surface modification and PEGylation of branched polyethyleneimine for improved biocompatibility. *J Appl Polym Sci*. 2013;128(6):3807-3813. https://doi.org/10.1002/app.38444
34. Jager M, Schubert S, Ochrimenko S, Fischer D, Schubert US. Branched and linear poly(ethylene imine)-based conjugates: synthetic modification, characterization, and application. *Chem Soc Rev*. 2012;41(13):4755-4767. https://doi.org/10.1039/c2cs35146c
35. Baglieri A, Vindrola D, Gennari M, Negre M. Chemical and spectroscopic characterization of insoluble and soluble humic acid fractions at different pH values. *Chem Biol Technol Agric*. 2014;1(9):1-11.
36. Camper AK. Involvement of humic substances in regrowth. *Int J Food Microbiol*. 2004;92(3):355-364. https://doi.org/10.1016/j.ijfoodmicro.2003.08.009
37. Wurzler N, Sobol O, Altmann K, Radnik J, Ozcan O. Preconditioning of AISI 304 stainless steel surfaces in the presence of flavins—Part I: effect on surface chemistry and corrosion behavior. *Mater Corros*. 2020;72:974-982. https://doi.org/10.1002/maco.202012191
38. Carlsson P, Segatto AZ, Granéli E. Nitrogen bound to humic matter of terrestrial origin - a nitrogen pool for coastal phytoplankton? *Mar Ecol Prog Ser*. 1993;97:105-116.
39. Delgado AV, González-Caballero F, Hunter RJ, Koopal LK, Lyklema J. Measurement and interpretation of electrokinetic phenomena. *J Colloid Interface Sci*. 2007;309(2):194-224. https://doi.org/10.1016/j.jcis.2006.12.075
40. Miller JH. *Experiments in Molecular Genetics*. Cold Spring Harbor Laboratory; 1972:466.
41. Hannig C, Follo M, Hellwig E, Al-Ahmad A. Visualization of adherent micro-organisms using different techniques. *J Med Microbiol*. 2010;59:1-7.
42. Amalric J, Mutin PH, Guerrero G, Ponche A, Sotto A, Lavigne JP. Phosphonate monolayers functionalized by silver thiolate species as antibacterial nanocoatings on titanium and stainless steel. *J Mater Chem*. 2009;19(1):141-149. https://doi.org/10.1039/b813344a
43. Grahame DAS, Olauson C, Lam RS, et al. Influence of chirality on the modes of self-assembly of 12-hydroxystearic acid in molecular gels of mineral oil. *Soft Matter*. 2011;7(16):7359–7365. https://doi.org/10.1039/c1sm05757j
44. Kowalik P, Elbaum D, Mikulski J, et al. Upconversion fluorescence imaging of HeLa cells using ROS generating SiO2-coated lanthanide-doped NaYF4 nanoconstructs. *RSC Adv*. 2017;7(48):30262-30273. https://doi.org/10.1039/c6ra25383k

45. Gawalt ES, Avaltroni MJ, Koch N, Schwartz J. Self-assembly and bonding of Alkanephosphonic acids on the native oxide surface of titanium. *Langmuir*. 2001;17:5736-5738.
46. Wapner K, Stratmann M, Grundmeier G. Structure and stability of adhesion promoting aminopropyl phosphonate layers at polymer/aluminium oxide interfaces. *Int J Adhes Adhes*. 2008;28(1–2):59-70. https://doi.org/10.1016/j.ijadhadh.2007.05.001
47. Luschtinetz R, Seifert G, Jaehne E, Adler H-JP. Infrared spectra of Alkylphosphonic acid bound to Aluminium surfaces. *Macromol Symp*. 2007;254(1):248-253. https://doi.org/10.1002/masy.200750837
48. Dai C, Liu N, Cao Y, Chen Y, Lu F, Feng L. Fast formation of superhydrophobic octadecylphosphonic acid (ODPA) coating for self-cleaning and oil/water separation. *Soft Matter*. 2014;10(40):8116-8121. https://doi.org/10.1039/c4sm01616e
49. Yudovin-Farber I, Beyth N, Weiss EI, Domb AJ. Antibacterial effect of composite resins containing quaternary ammonium polyethyleneimine nanoparticles. *J Nanopart Res*. 2009;12(2):591-603. https://doi.org/10.1007/s11051-009-9628-8
50. Qin X, Liu F, Wang G, Huang G. Adsorption of humic acid from aqueous solution by hematite: effects of pH and ionic strength. *Environ Earth Sci*. 2014;73(8):4011-4017. https://doi.org/10.1007/s12665-014-3686-7
51. Elzinga EJ, Huang JH, Chorover J, Kretzschmar R. ATR-FTIR spectroscopy study of the influence of pH and contact time on the adhesion of *Shewanella putrefaciens* bacterial cells to the surface of hematite. *Environ Sci Technol*. 2012;46(23):12848-12855. https://doi.org/10.1021/es303318y
52. Baier RE. Surface behaviour of biomaterials: the theta surface for biocompatibility. *J Mater Sci Mater Med*. 2006;17(11):1057-1062. https://doi.org/10.1007/s10856-006-0444-8
53. Liu C, Zhao Q, Liu Y, Wang S, Abel EW. Reduction of bacterial adhesion on modified DLC coatings. *Colloids Surf B Biointerfaces*. 2008;61:182-187.

SUPPORTING INFORMATION

Additional supporting information may be found online in the Supporting Information section at the end of this article.

How to cite this article: Wurzler N, Hidde G, Schenderlein M, Ozcan O. Effect of organic conditioning layers adsorbed on stainless steel AISI 304 on the attachment and biofilm formation of electroactive bacteria *Shewanella putrefaciens* CN32. *Engineering Reports*. 2022;4(1):e12458. doi: 10.1002/eng2.12458